EWS-FLI-1 Expression Triggers a Ewing's Sarcoma Initiation Program in Primary Human Mesenchymal Stem Cells

Nicolò Riggi,[1] Mario-Luca Suvà,[1] Domizio Suvà,[3] Luisa Cironi,[1] Paolo Provero,[4] Stéphane Tercier,[2] Jean-Marc Joseph,[2] Jean-Christophe Stehle,[1] Karine Baumer,[1] Vincent Kindler,[3] and Ivan Stamenkovic[1]

[1]Division of Experimental Pathology, Institute of Pathology, and [2]Department of Pediatric Surgery, University of Lausanne, Lausanne, Switzerland; [3]Department of Orthopedics, University of Geneva, Geneva, Switzerland; and [4]Department of Genetics Biology and Biochemistry, University of Turin, Turin, Italy

Abstract

Ewing's sarcoma family tumors (ESFT) express the *EWS-FLI-1* fusion gene generated by the chromosomal translocation t(11;22)(q24;q12). Expression of the EWS-FLI-1 fusion protein in a permissive cellular environment is believed to play a key role in ESFT pathogenesis. However, EWS-FLI-1 induces growth arrest or apoptosis in differentiated primary cells, and the identity of permissive primary human cells that can support its expression and function has until now remained elusive. Here we show that expression of EWS-FLI-1 in human mesenchymal stem cells (hMSC) is not only stably maintained without inhibiting proliferation but also induces a gene expression profile bearing striking similarity to that of ESFT, including genes that are among the highest ESFT discriminators. Expression of EWS-FLI-1 in hMSCs may recapitulate the initial steps of Ewing's sarcoma development, allowing identification of genes that play an important role early in its pathogenesis. Among relevant candidate transcripts induced by EWS-FLI-1 in hMSCs, we found the polycomb group gene *EZH2*, which we show to play a critical role in Ewing's sarcoma growth. These observations are consistent with our recent findings using mouse mesenchymal progenitor cells and provide compelling evidence that hMSCs are candidate cells of origin of ESFT. [Cancer Res 2008;68(7):2176–85]

Introduction

Ewing's sarcoma is the second most common bone malignancy in children and young adults with a peak incidence between the ages of 14 and 20 years. It is associated with specific chromosomal translocations that lead to the formation of fusion genes encoding proteins composed of the transactivation domain of EWS and the DNA binding domain (DBD) of one of five ETS family transcription factors, including *FLI1, ERG, ETV1, ETV4*, and *FEV*. More than 85% of Ewing's sarcoma family tumors (ESFT) are associated with the chromosomal translocation t(11;22)(q24;q12) that generates the *EWS-FLI-1* fusion gene (1). The corresponding fusion protein is believed to behave as an aberrant transcription factor that transforms target cells by deregulating their gene expression program.

Among the functions that have been ascribed to the EWS-FLI-1 protein is the regulation of target cell differentiation. EWS-FLI-1 expression induces immunohistologic ESFT features in several immortalized and malignant cell types (2–6) and recent observations have shown that numerous genes involved in neural differentiation and neuroectodermal development that are expressed in ESFT cell lines are regulated by EWS-FLI-1 (7–10). It is also well established that EWS-FLI-1 possesses oncogenic properties. Its expression can accelerate tumorigenesis of murine NIH 3T3 cells in immunocompromised mice (6, 11), whereas its repression by antisense constructs or specific siRNA sequences in human ESFT cell lines results in decreased cell growth *in vitro* and tumorigenicity *in vivo* (12, 13). Introduction of EWS-FLI-1 into heterologous cells and fusion protein expression knockdown in ESFT cell lines have led to the identification of several candidate EWS-FLI-1 target genes that may be implicated in transformation and/or tumor progression (refs. 10, 14; reviewed in ref. 15). However, EWS-FLI-1 function is highly cell context dependent, and the identification of the genes implicated in the initiating phase of ESFT development may elude approaches using established heterologous cell lines and cells derived from late-stage ESFT. Full elucidation of ESFT pathogenesis requires understanding of the tumor initiating program induced by EWS-FLI-1 and identification of primary target cells that are permissive for its expression.

Efforts to identify candidate primary cells that constitute the origin of ESFT and that could help recapitulate the very first steps of tumor formation have been hampered by EWS-FLI-1 toxicity. Thus, introduction of EWS-FLI-1 into mouse embryonic fibroblasts resulted in cell cycle arrest and cell death (16). Mouse embryonic fibroblasts from $p19^{ARF-/-}$ mice transfected with EWS-FLI-1 were observed to maintain EWS-FLI-1 expression but did not form tumors *in vivo* (16). Only on transformation with SV40 T antigen could EWS-FLI-1–expressing mouse embryonic fibroblasts lacking $p19^{ARF}$ or p53 form tumors *in vivo* that display histologic features resembling those of human Ewing's sarcoma (16). Similar observations were made in hTERT-immortalized human primary fibroblasts where EWS-FLI-1 expression induced p53-mediated growth arrest and apoptosis (17). However, at least half of Ewing's sarcomas seem to have a functional p53 pathway and to retain $p19^{ARF}$ expression (18), suggesting the existence of primary cells that are permissive for EWS-FLI-1 expression without triggering an oncogenic stress type response that results in cell cycle arrest.

Recently, introduction of EWS-FLI-1 into unsorted murine bone marrow–derived cells was observed to result in the formation of tumors displaying various phenotypes including that of Ewing's sarcoma (19). Work from our own laboratory has shown that primary mouse bone marrow–derived mesenchymal progenitor cells undergo transformation as a result of stable EWS-FLI-1 expression

Note: N. Riggi, M-L. Suvà, and D. Suvà contributed equally to this work.

Supplementary data for this article are available at Cancer Research Online (http://cancerres.aacrjournals.org/).

Requests for reprints: Ivan Stamenkovic, Experimental Pathology, University of Lausanne, Lausanne, Switzerland. Phone: 41-21-314-7136; Fax: 41-21-314-7110; E-mail: Ivan.Stamenkovic@chuv.ch.

doi:10.1158/0008-5472.CAN-07-1761

(20). Mouse mesenchymal progenitor cells expressing EWS-FLI-1 displayed robust up-regulation of insulin-like growth factor 1 (IGF-I), which is believed to play a major role in ESFT development, and on *in vivo* injection, formed tumors composed predominantly of sheets of small round cells, consistent with the ESFT phenotype (20). The tumors displayed high sensitivity to IGF-I receptor (IGF-IR) inhibition, a hallmark of Ewing's sarcoma, as well as expression of Ewing's sarcoma-associated markers including neural specific enolase and CD99 (20).

Based on these observations, we addressed the possibility that human mesenchymal stem cells (hMSC) might provide a permissive cellular environment for EWS-FLI-1. Introduction of the fusion gene into bone-derived hMSCs resulted in its stable expression as well as phenotypic and transcriptional changes that reflect key features of Ewing's sarcoma. Among the observed transcriptional changes was the induction of the polycomb group gene enhancer of zeste homolog 2 (*EZH2*), which is reported to be highly expressed in Ewing's sarcoma (21) and proposed to be implicated in cancer development, stem cell maintenance, and proliferation (22). Partial suppression of EZH2 in two different Ewing's sarcoma cell lines resulted in a dramatic reduction of their proliferation and tumorigenic potential, suggesting that EZH2 may be an important player in ESFT initiation and growth.

Materials and Methods

Cell culture. Human MSCs were obtained from femoral head bone marrow of seven adult patients undergoing total hip replacement as previously described (23). MSCs were cultured at low confluence in Iscove's modified Dulbecco's medium, 10% FCS, and 10 ng/mL platelet-derived growth factor BB (PeProtech EC) and were tested for multilineage differentiation into adipocytes, chondrocytes, and osteoblasts (24). SK-N-MC and A673 cell lines (American Type Culture Collection) were cultured in RPMI 1640 containing 10% FCS.

Cloning and reverse transcription-PCR. The cDNA clone encoding the human *EWS-FLI-1* type 2 fusion gene was amplified from the SK-N-MC Ewing sarcoma cell line, and cloned with or without a V5 tag at its 3′end in the pMSCV Puro retroviral vector (BD Biosciences Clontech) as previously described (20). The EWS-FLI-1 R340N DBD mutant (DBDM) was amplified by PCR using the wild-type (wt) sequence as template, with the following primers: hEWS forward *Xho*I, CCGCTCGAGCCACCATGGCGTCCACGGATTACAG; hFLI-1 reverse R340N, ATCATAGTAATAATTGAGGGCCCGGCTCAGCTTGTC; hFLI-1 forward R340N, CGACAAGCTGAGCCGGGCCCTCAATTATTACTATGA; and V5 reverse *Hpa*I (including a stop codon), GTTAACTCACGTAGAATCGAGACCGAGGAGAGGGTTAGGGATAGGCTTACC.

The amplified fragment was *Xho*I-*Hpa*I digested, inserted into the pMSCV Puro retroviral expression vector, and sequenced to verify the presence and integrity of the inserted cDNA.

Retroviral infection. Expression of EWS-FLI-1V5 and DBDM in hMSCs was achieved using Retroviral Gene Transfer and Expression (BD Biosciences Clontech) according to the manufacturer's recommendations. Expression of the fusion genes and corresponding proteins was tested at each time point in all the four batches of cells by reverse transcription-PCR and Western blot analysis with the mouse anti-V5 antibody, respectively. Infected cells were selected with 0.75 μg/mL puromycin for 5 d and the bulk of the resistant cells was used in subsequent experiments.

Western blot. Cell lysis, SDS-PAGE, blotting, and immunostaining were done by standard procedures and protein bands were detected with a chemiluminescent substrate kit (Pierce) according to the manufacturer's recommendations. Primary mouse anti–V5 epitope monoclonal antibody (mAb; Invitrogen), mouse anti-CD99 mAb (Signet Laboratories), mouse anti-FLI1 mAb (BD PharMingen), mouse anti–β-actin (Sigma), and rabbit anti-EZH2 polyclonal (Cell Signaling) antibodies were used. Secondary antibodies were horseradish peroxidase–conjugated goat anti-mouse (Bio-Rad) and mouse anti-rabbit (Sigma) IgG.

Immunohistochemistry and flow cytometry. For *in vitro* staining, cells were fixed for 20 min at room temperature with 4% paraformaldehyde in 24-well plates. The primary antibodies used were polyclonal rabbit anti-TAU (1:200 dilution; Sigma) and mouse anti-NGFR hybridoma (kindly provided by Dr. Nicole Gross, Centre Hospitalier Universitaire Vaudois, Lausanne, Switzerland). Paraffin-embedded sections of primary Ewing's sarcoma, SK-N-MC, and A673 derived tumors were stained with rabbit anti-human EZH2 polyclonal antibody (1:50 dilution; Cell Signaling). Horseradish peroxidase staining was done with biotin-conjugated horse anti-mouse or goat anti-rabbit immunoglobulin (Vector Laboratories) and revealed with a DAKO DAB Kit.

Pellets of hMSCs differentiated in the chondrogenic lineage were frozen in optimum cutting temperature compound (Tissue-Tek, Sakura Finetek), cut into 5-μm-thick sections, and stained with anti–collagen type II antibody (clone II-II6B3 mouse IgG1, 1:2 dilution; Developmental Studies Hybridoma Bank, University of Iowa) as described (23).

Flow cytometry analysis of hMSCs was done as previously described (24). Additional antibodies used in this study included anti–STRO-1 (Invitrogen) and anti-CD106-phycoerythrin (BD PharMingen).

Affymetrix microarray, quantitative real-time PCR analysis, and EZH2 knockdown are discussed in Supplementary data.

Results

Expression of EWS-FLI-1 alters the hMSC phenotype. Human MSCs were maintained at low confluence and tested for their ability to differentiate into adipocytes, chondrocytes, and osteocytes in response to appropriate cytokines (refs. 23, 24; Fig. 1*A, left*). In addition to maintaining their differentiation potential, the cells displayed a homogeneous CD45-, CD19-, CD34-, CD11b-, CD80-, CD86-, and CD14-negative and a CD105- and CD90-positive phenotype, consistent with that of MSCs (Fig. 1*A, right*). These cells were also positive for CD106 and STRO-1 (Supplemental data 1*A*), as reported in the litterature (25). Their *in vitro* life span was ~3 months (23). A pMSCV retroviral vector containing a V5 sequence–tagged EWS-FLI-1 cDNA, a V5 sequence–tagged cDNA encoding the R340N EWS-FLI-1 DBDM, or no extraneous DNA (empty vector) was used to produce the corresponding viruses and infect four independent batches of hMSCs that had undergone 8 population doublings. The EWS-FLI-1 fusion protein bearing the R340N has been shown to lack DNA binding activity while retaining some degree of transforming potential (25). EWS-FLI-1 and DBDM expression was tested by Western blot analysis with the anti-V5 antibody at various time points following infection. Expression of both the wt and DBDM EWS-FLI-1 fusion proteins was observed 24 hours after infection and was found to be stably maintained several weeks later in all samples [Fig. 1*B* (*left*) and *D* (*right*), and data not shown]. Moreover, the fusion protein expression level in two different batches of EWS-FLI-1–infected hMSCs was comparable to that of Ewing sarcoma cell lines, as assessed by Western blot analysis with the anti-FLI1 antibody (Fig. 1*B, right*).

Human MSCs expressing EWS-FLI-1 ($hMSC^{EWS\text{-}FLI\text{-}1}$) underwent a marked morphologic change, displaying a round instead of the typically elongated, spindle shape of their wt, empty vector–, and DBDM ($hMSC^{DBDM}$)–expressing counterparts (Fig. 1*C*), whereas their *in vitro* life span, viability, and proliferation rate remained unaltered as assessed by an MTT assay (Fig. 2*A* and data not shown). The change in morphology of $hMSC^{EWS\text{-}FLI\text{-}1}$ was consistent with the reported ability of EWS-FLI-1 to modify the differentiation program of mouse mesenchymal progenitor cells (26). Because CD99 is the most reliable, although not specific, marker of ESFT, we addressed the possibility that EWS-FLI-1 expression induces CD99 in hMSCs. Western blot analysis with an

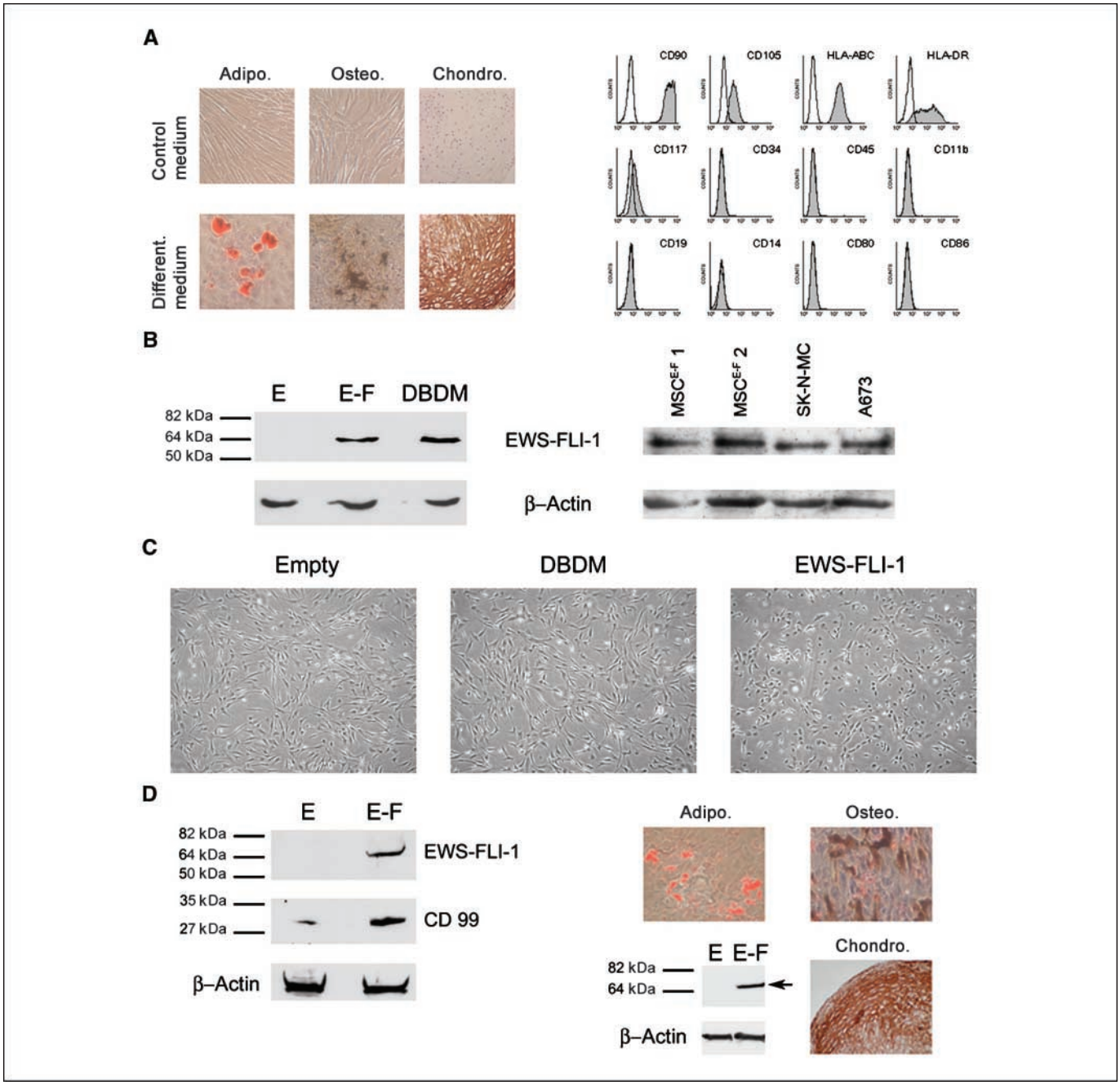

Figure 1. hMSCs stably express the EWS-FLI-1 fusion protein, display morphologic changes *in vitro*, and retain their differentiation plasticity. *A, left,* hMSCs retain the ability to differentiate into adipogenic, osteogenic, and chondrogenic lineages when stimulated with the appropriate cytokines (see Materials and Methods for details). *Bottom,* adipocytic differentiation, oil Red-O staining (control: medium only); osteoblastic differentiation, von Kossa staining (control: medium only); and chondrocytic differentiation, anti–collagen type II labeling counterstained with hematoxylin (control: secondary antibody alone). Magnification: adipocytes and osteocytes, ×200; chondrocytes, ×100. *Right,* FACS analysis of the hMSC phenotype. Cells were labeled with phycoerythrin-conjugated antibodies against CD45, CD117, CD19, CD14, CD80, CD86, HLA-ABC, CD105, CD11b, CD34, CD90, and HLA-DR or with isotype-matched control antibodies. *White area,* control antibody; *gray area,* specific antibody. *B, left,* Western blot analysis of EWS-FLI-1 (*E-F*) and DBDM expression in hMSCs 12 d after infection (*E,* empty vector–infected cells); *right,* comparison of the fusion protein expression in lysates of equal numbers of two EWS-FLI-1–infected hMSC batches and the two Ewing sarcoma cell lines, SK-N-MC and A673. *C,* $hMSC^{EWS\text{-}FLI\text{-}1}$ underwent marked morphologic changes *in vitro*, adopting a round, rather than the elongated, phenotype of their empty vector–infected and DBDM-expressing counterparts. *D, left,* CD99 induction by EWS-FLI-1 in $hMSC^{EWS\text{-}FLI\text{-}1}$ (*E-F*) compared with empty vector–infected cells (*E*), as assessed by Western blot analysis; *right,* $hMSC^{EWS\text{-}FLI\text{-}1}$ retain the expression of the fusion protein 4 wk following infection (*arrow*) and the ability to differentiate into the three lineages described in *A*. Magnification: adipocytes and osteocytes, ×200; chondrocytes, ×100.

anti-CD99 antibody showed that hMSCs constitutively express low levels of CD99 and that its expression is strongly induced by EWS-FLI-1 (Fig. 1*D, left*). Interestingly, when hMSCs were tested for their ability to differentiate toward the chondrocytic, osteocytic, and adipocytic lineages 4 weeks after infection, they were observed to conserve their differentiation potential despite expression of EWS-FLI-1 (Fig. 1*D, right*). Three independent batches of hMSCs expressing EWS-FLI-1 were subjected to lineage-specific, differentiation-inducing culture conditions, and all displayed trilineage differentiation ability.

hMSC$^{EWS\text{-}FLI\text{-}1}$ display induction of genes implicated in neural differentiation and neuroectodermal development as well as that of known EWS-FLI-1 target genes. Total RNA was extracted 12 days after infection and selection from each of the four EWS-FLI-1–, DBDM-, and empty vector–containing hMSC batches, and the corresponding mRNA was used to perform gene expression profile analysis using the Affymetrix U133 Plus 2.0 Arrays. Statistical analysis, using rank products (27) and a false discovery rate of 1%, revealed 614 and 262 probe sets corresponding to 393 and 174 genes to be respectively induced and repressed in hMSC$^{EWS\text{-}FLI\text{-}1}$ compared with empty vector–infected counterparts, whereas 104 and 158 genes were respectively up-regulated and down-regulated in hMSC^{DBDM} (Supplementary data 2). Importantly, all four batches of hMSC$^{EWS\text{-}FLI\text{-}1}$ cells revealed an almost identical gene expression profile, as shown by the heat map in Supplementary data 1B where the expression profile of the four samples is compared with that of cells infected with the R340N DBDM.

Among the most potently induced transcripts in hMSC$^{EWS\text{-}FLI\text{-}1}$ were genes encoding proteolytic enzymes (primarily matrix

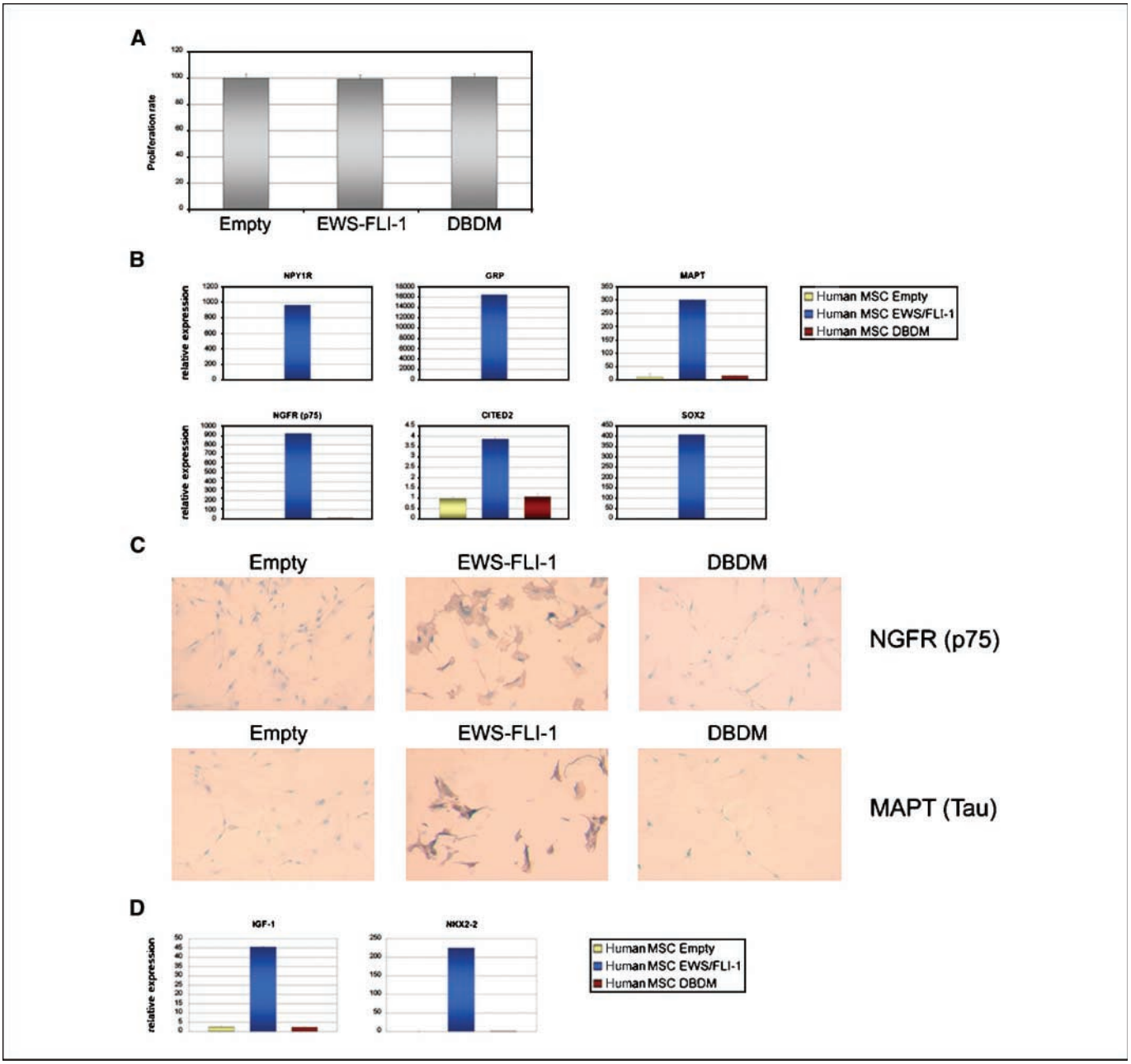

Figure 2. EWS-FLI-1 does not alter hMSC proliferation and induces a neuroectodermal gene expression profile. *A,* MTT assay analysis of the proliferation rate of hMSCs expressing DBDM or EWS-FLI 1 compared with their empty vector–infected counterparts. *B,* comparison of the induction in hMSC$^{EWS\text{-}FLI\text{-}1}$ and hMSC^{DBDM} of selected neuroectodermal markers from the list shown in Table 1*A*, as assessed by real-time PCR. *C,* NGFR and MAPT genes were selected from *B* to further characterize their induction at the protein level by *in vitro* staining of hMSC$^{EWS\text{-}FLI\text{-}1}$ compared with their empty vector– and DBDM-infected counterparts. Magnification, ×200. *D,* the induction of the two candidate EWS-FLI-1 target genes, *IGF-I* and *NKX2-2*, was confirmed by real-time PCR. All real-time PCR experiments were normalized to cyclophyllin A and done in triplicate. *Columns,* mean of three independent determinations.

metalloproteinases), adhesion receptors (including *CLDN1, ICAM1, PCDH7/17, CEACAM1*, and *CDH11)*, and growth factors (including *IGF1, TGFA/B*, and *HBEGF*; Supplementary data 1C). Induction of these genes is consistent with the alterations in growth, survival, adhesion/migration, and tissue remodeling potential that may be expected in cells undergoing transformation.

EWS-FLI-1 expression in hMSCs also induced numerous genes that encode neural cell markers or that are implicated in neural crest development and neuronal differentiation, including *NYP1R, GRP, MSX1, EGR2, NKX2-2, NGFR, CITED2, CDH11*, and *MAPT* (Table 1*A*). Because expression of these genes is consistent with the primitive neuroectodermal phenotype of ESFT, six of them, including *NPY1R, GRP, MAPT, NGFR, CITED2*, and *SOX2*, were selected for validation of their observed expression change. Up-regulation of all six genes in $hMSC^{EWS\text{-}FLI\text{-}1}$ was confirmed by quantitative real-time PCR (Fig. 2*B*). To assess the importance of DNA binding of EWS-FLI-1 in the induction of these six candidate target genes, their expression was assessed in MSCs infected with the EWS-FLI-1 mutant bearing the R340N loss-of-function mutation in the DBD of FLI-1. Quantitative real-time PCR analysis revealed that hMSCs expressing the mutated EWS-FLI-1 ($hMSC^{DBDM}$) failed to display induction of any of the genes, suggesting that an intact DBD is required for EWS-FLI-1–mediated regulation of their expression (Fig. 2*B*). To further validate the neuroectodermal phenotype induced by EWS-FLI-1, we assessed NGFR and MAPT protein expression in hMSCs infected with the three retroviral vectors. Consistent with the gene expression profile, strong induction of both neural markers was observed in $hMSC^{EWS\text{-}FLI\text{-}1}$, but not in empty vector– or DBDM-infected counterparts (Fig. 2*C*). The robust induction of NGFRp75 by EWS-FLI-1 was further confirmed by fluorescence-activated cell sorting (FACS) analysis of the infected cells (Supplementary data 1E).

Many of the reported candidate EWS-FLI-1 target genes were induced in $hMSC^{EWS\text{-}FLI\text{-}1}$, including *ID2, IGF1, MMP1, TNC, COL11A1*, and *UPP1* (20, 28–30), as well as the more recently identified targets *NROB1* and *NKX2-2* (refs. 7, 10; Table 1*A*). Whereas up-regulation of several of these genes by EWS-FLI-1 has been observed in a variety of cellular backgrounds, induction of *IGF-I* has thus far been detected only in mouse mesenchymal progenitor cells (20). Ewing's sarcoma cells are highly sensitive to IGF-IR blockade, consistent with the possibility that IGF-I may facilitate EWS-FLI-1–mediated transformation and promote ESFT cell survival, particularly in the early phases of ESFT development. The relationship between EWS-FLI-1 and *NKX2-2* was recently discovered using an inducible rescue approach in ESFT cell lines (10), and expression of the *NKX2-2* gene has been suggested to be relevant to both ESFT differentiation and pathogenesis (10). Quantitative real-time PCR analysis confirmed induction of both *IGF1* and *NKX2-2* genes in $hMSC^{EWS\text{-}FLI\text{-}1}$ cells but not in $hMSC^{DBDM}$ cells (Fig. 2*D*), indicating that regulation of both genes by EWS-FLI-1 requires integrity of the DBD of FLI-1. Transcript levels of a panel of Ewing's sarcoma discriminating genes in $MSC^{EWS\text{-}FLI\text{-}1}$ were compared with those of the same genes in a fresh primary Ewings' sarcoma sample. Several of the transcripts, particularly *NPY1R, GRP, EZH2*, and *IGF1*, were found to be expressed at comparable levels in $MSC^{EWS\text{-}FLI\text{-}1}$ and primary Ewing's sarcoma cells (Supplementary data 1D).

The expression profile of $hMSC^{EWS\text{-}FLI\text{-}1}$ closely mimics that of ESFT but not of other bone and soft tissue tumors. To assess the degree of relatedness of the hMSC model to ESFT, we compared the gene expression profile of $MSC^{EWS\text{-}FLI\text{-}1}$ to those of

Table 1. EWS-FLI-1–induced differentiation markers and candidate target genes

Clone	*M* value	Gene symbol
(*A*) Neuroectodermal differentiation markers		
205440_s_al	7.004544088	*NPY1R*
217561_at	5.506065541	*CALCA*
203413_at	4.293524987	*NELL2*
206915_at	4.205361231	*NKX2-2*
214636_at	3.667256337	*CALCB*
236088_at	3.503590436	*NTNG1*
228038_at	3.400729183	*SOX2*
201565_s_at	2.792584692	*ID2*
204105_s_at	2.571239931	*NRCAM*
205932_s_at	2.652991206	*MSX1*
1554485_s_at	2.655283127	*TMEM37*
213479_at	2.366643943	*NPTX2*
218162_at	2.249141903	*OLFML3*
205249_at	2.243181602	*EGR2*
230303_at	2.39988201	*SYNPR*
208605_s_at	2.227463845	*NTRK1*
39966_at	2.222217226	*CSPG5*
204869_at	2.146557475	*PCSK2*
221933_at	1.982400408	*NLGN4X*
203929_s_at	1.659102536	*MAPT*
232226_at	1.62194636	*LRRC4C*
205858_at	1.528171209	*NGFR*
207980_s_at	1.461895211	*CITED2*
227933_at	1.209141398	*LRRN6A*
Candidate EWS-FLI-1 target genes		
205440_s_at	7.004544088	*NPY1R*
206915_at	4.205361231	*NKX2-2*
204475_at	3.88747653	*MMP1*
201565_s_at	2.792584692	*ID2*
209541_at	2.366028399	*IGF1*
201645_at	1.576763978	*TNC*
37892_at	1.434881719	*COL11A1*
203234_at	1.46967763	*UPP1*
(*B*) Staege ESFT signature and hMSC EWS-FLI-1 common genes		
205440_s_at	7.004544088	*NPY1R*
202746_at	6.728787172	*ITM2A*
219908_at	4.691662572	*DKK2*
203358_s_at	3.103715832	*EZH2*
228636_at	2.688202743	*BHLHB5*
1552610_a_at	2.165365299	*JAK1*
205249_al	2.243181602	*EGR2*
225871_at	2.188749054	*STEAP2*
219528_s_at	1.988302947	*BCL11B*
206812_at	1.359914681	*ADRB3*
241946_at	1.313478058	*ZDHHC21*
226106_at	1.192636061	*RNF141*
227933_at	1.209141398	*LRRN6A*
219825_at	1.544188607	*CYP26B1*

NOTE: (*A*) Summary of genes implicated in neural differentiation and neuroectodermal development, as well as known EWS-FLI-1 target genes, found to be part of the hMSC EWS-FLI-1 gene expression profile. Log 2 *m* values of fold induction are shown. (*B*) List of the 14 common genes between hMSC EWS-FLI-1 and the ESFT expression signature published by Staege et al. (21). Log 2 *m* values of fold induction are shown.

Ewing's sarcoma and other bone and soft tissue tumors in a recently established sarcoma gene expression database (31). A remarkable similarity was found between the gene expression profile of hMSC$^{EWS\text{-}FLI\text{-}1}$ and that of Ewing's sarcoma samples. Of the 225 genes proposed to be ESFT discriminators, 40 were observed to be induced in hMSC$^{EWS\text{-}FLI\text{-}1}$ (Fig. 3*C*), compared with an expected number of 4.46 (P = 1.95e−25). To determine whether hMSC$^{EWS\text{-}FLI\text{-}1}$ display comparable or greater similarity to ESFT than fibroblast$^{EWS\text{-}FLI\text{-}1}$ (17), direct comparison of each gene expression profile was made to that of native ESFT (31). To do so, only the genes found to be present in all three arrays were used, which resulted in 94 genes in the fibroblast profile list and 235 genes in the MSC profile list. This approach revealed that of the 94 genes in the fibroblast profile list, 14 were common to the native ESFT list, for an expected 1.77 (P = 2.0e−9); of 235 genes in the hMSC list, 29 were common to the ESFT list, for an expected 4.43 (P = 3.8 E-16). These observations suggest that fibroblasts provide a more restrictive environment than hMSCs for expression of the target gene repertoire of the EWS-FLI-1 fusion protein (17).

Importantly, genes that were induced in hMSC$^{EWS\text{-}FLI\text{-}1}$, including *FVT1, DKK2, MAPT, PRKCB1, JAK1, ITM2A, FRZB, CITED2, STEAP1, STEAP2*, and *ID2*, were among the top discriminators for Ewings' sarcoma (Fig. 3*C*). Among the 12 other sarcomas analyzed, only dermatofibrosarcoma protuberans displayed a gene expression

A

Tumor type	Baird genes	hMSC$^{E\text{-}F}$ genes	Expected overlap	Observed overlap	*P* value
EWS	225	393	4 46	40	1 95 E-25
DFSP	177	393	3 51	11	0 011
LIPO	170	393	3 37	9	0 091
RMS	149	393	2 95	6	1
MFH	281	393	5 57	9	1
OS	109	393	2 16	4	1
HPC	192	393	3 81	6	1
GIST	236	393	4 68	7	1
LMS	185	393	3 67	5	1
SS	146	393	2 9	4	1
MULL	109	393	2 16	2	1
MPNST	135	393	2 68	2	1
FIBRO	83	393	1 65	1	1

B

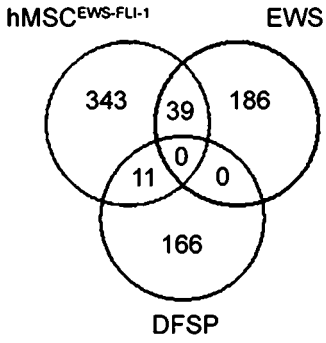

C

Clone	*M* value	Gene symbol
Baird EWS - hMSC EWS-FLI-1 common genes		
202746_at	6 728787172	*ITM2A* *
209685_s_at	6 034420429	*PRKC81* *
223557_s_at	5 945961124	*TMEFF2*
206002_at	5 825437121	*GPR64* *
1554384_at	5 692775889	*PADI2*
219908_at	4 691662572	*DKK2* *
206326_at	3 719512035	*GRP*
215695_s_at	3 320845668	*GYG2* *
1558279_a_at	3 213378391	*FVT1* *
206481_s_at	3 194102816	*LDB2*
218831_s_at	2 945345607	*FCGRT*
201565_s_at	2 792584692	*ID2* *
201563_at	2 699107386	*SORD*
204201_s_at	2 696283214	*PTPN13*
203139_at	2 569102173	*DAPK1*
203697_at	2 47511083	*FRZB* *
218976_at	2 413864833	*DNAJC12*
213552_at	2 202135681	*GLCE*
225871_at	2 188749054	*STEAP2*
1552610_a_at	2 165365299	*JAK1* *
220948_s_at	2 044269192	*ATP1A1* *
205227_at	2 021621858	*IL1RAP*
205066_s_at	1 932401389	*ENPP1*
205771_s_at	1 919873962	*AKAP7*
225263_at	1 907467558	*HS6ST1*
203606_at	1 729965997	*ALDHSA1*
216080_s_at	1 682842935	*FADS1*
203929_s_at	1 659102536	*MAPT* *
244350_at	1 608714637	*MYO10*
207980_s_at	1.461895211	*CITE02* *
227102_at	1 428571222	*TRIM35*
204687_at	1 410829519	*PARM1_HUMAN*
205542_at	1 300299474	*STEAP1* *
206655_s_at	1 240558574	*SEPT*
226208_at	1 213191727	*ZSWM6*
226106_at	1 192636061	*RNF141*
211340_s_at	1 173894961	*MCAM*
212402_at	1 164013889	*ZC3H13*
235003_at	1 162274498	*UHMK1*
231714_s_at	1 152443048	*AP4B1*

D

Tumor type	Baird genes	hMSC^{DBDM} genes	Expected overlap	Observed overlap	*P* value
EWS	225	104	1 18	0	1
DFSP	177	104	0 92	2	1
LIPO	170	104	0 89	1	1
RMS	149	104	0 78	4	0 11
MFH	281	104	1 47	2	1
OS	109	104	0 57	0	1
HPC	192	104	0 90	1	1
GIST	236	104	1 23	2	1
LMS	185	104	0 97	3	1
SS	146	104	0 77	1	1
MULL	109	104	0 57	1	1
MPNST	135	104	0 57	2	1
FIBRO	83	104	0 43	0	1

Figure 3. EWS-FLI-1 expression in hMSCs induces a gene expression profile that closely mimics that of ESFT but not of other bone and soft tissue tumors. *A,* statistical analysis of the genes common to hMSC$^{EWS\text{-}FLI\text{-}1}$ and a publicly available database of soft tissue tumor gene expression profile [Baird et al. (31)], showing the striking similarity of hMSC$^{EWS\text{-}FLI\text{-}1}$ to ESFT but not to other sarcomas, with the significant *P* values indicated. *B,* Venn diagram representation of hMSC$^{EWS\text{-}FLI\text{-}1}$ profile relatedness to ESFT, dermatofibrosarcoma protuberans, and myxoid liposarcoma, based on the number of shared genes in their respective profiles, as showed in *A*. *C,* list of the 40 genes found to be shared by the hMSC$^{EWS\text{-}FLI\text{-}1}$ and ESFT gene expression profiles. *Asterisks,* genes found by Baird et al. to be top discriminators for Ewing's sarcoma. Log 2 *m* values of fold induction are shown. *D,* statistical analysis of the genes common to hMSC^{DBDM} and the same tumor database used in *A*, indicating that expression of the EWS-FLI-1 DBDM in hMSCs does not induce a gene expression profile in the infected cells that can discriminate ESFTs from other sarcomas. *EWS,* Ewing's sarcoma; *DFSP,* dermatofibrosarcoma protuberans; *LIPO,* liposarcoma; *RMS,* rhabdomyosarcoma; *MFH,* malignant fibrous histiocytoma; *OS,* osteosarcoma; *HPC,* hemangiopericytoma; *GIST,* gastrointestinal stromal tumor; *LMS,* leiomyosarcoma; *SS,* synovial sarcoma; *MULL,* mixed mullerian; *MPNST,* malignant peripheral nerve sheath tumor; *FIBRO,* fibrosarcoma.

profile with marginal similarity to hMSC$^{EWS\text{-}FLI\text{-}1}$ (P = 0.011) (Fig. 3*A* and *B*). The same statistical analysis was applied to the gene expression profile of hMSC^{DBDM}. In contrast to wt EWS-FLI-1, expression of the EWS-FLI-1 mutant form did not confer on MSCs any statistically significant similarity with Ewing sarcoma (Fig. 3*D*). This observation supports the notion that the lack of shape change displayed by the hMSC^{DBDM} *in vitro* reflects a different genetic program in these cells, and highlights the importance of DNA binding for the ESFT phenotype–inducing properties of the fusion protein.

The highly discriminating ability of the hMSC$^{EWS\text{-}FLI\text{-}1}$ gene expression profile for ESFTs was further confirmed by another study, which assessed the transcriptome of a broad range of mesenchymal tumors and identified the *CALCB, MAPT*, and *PRKCB1* genes as prominent Ewing's sarcoma discriminators (32), all of which we found to be induced in hMSC$^{EWS\text{-}FLI\text{-}1}$ (Table 1; Supplementary data 2).

Comparison of the genes induced in hMSC$^{EWS\text{-}FLI\text{-}1}$ with a set of 38 genes (of which only 34 were included on our microarray) found to be up-regulated in ESFT with respect to a wide spectrum of normal tissues and neuroblastomas (21) revealed 14 shared genes (P = 1.12e−15), including the strong ESFT discriminators *NPYR1, ITM2A, DKK2, JAK1, STEAP*, and *EGR2* (Table 1*B*). Moreover, of a subset of 19 transcripts from the 34-gene set that could clearly distinguish an ESFT cell line (SK-N-MC) from neuroblastoma cell lines (21), 8 were part of the hMSC$^{EWS\text{-}FLI\text{-}1}$ profile, whereas none of the transcripts in the 34-gene set were identified in the hMSC^{DBDM} expression profile (expected 0.18, P = 1.00). The same study reported that introduction of EWS-FLI-1 into HEK 293 cells induced only one gene of this subset, namely, *CCND1*, further highlighting the selective permissiveness of hMSCs for EWS-FLI-1 function (21).

Injection of hMSC$^{EWS\text{-}FLI\text{-}1}$ into immunocompromised mice. Following injection into the subcapsular renal compartment of immunocompromised mice, hMSC$^{EWS\text{-}FLI\text{-}1}$ did not form tumors, suggesting that despite expressing many of the hallmarks of ESFT, these cells require some additional event to become tumorigenic in mice. This observation is not surprising in the sense that whereas there have been several examples of a single genetic event transforming mouse progenitor cells (20, 33–35), recent evidence suggests that five events are required to transform human MSCs (36). By analogy to the present study, TLS-ERG and TEL-JAK2 respectively initiated a leukemogenic program and erythropoietin-independent erythropoiesis in normal human hematopoietic cells but fell short of rendering them tumorigenic *in vivo* (37, 38).

EZH2 promotes Ewing's sarcoma growth. Among transcripts that were up-regulated in hMSC$^{EWS\text{-}FLI\text{-}1}$, we identified the gene encoding EZH2, a member of the polycomb group proteins (Supplementary data 2), which has recently been found to be expressed in ESFT (21). Together with EED and SUZ12, EZH2 forms the polycomb-repressive complex 2, believed to be a key regulator of embryonic development, stem cell renewal, and differentiation (39, 40). EZH2 is the catalytically active component of polycomb-repressive complex 2 and is believed to silence target genes by acting as a methyltransferase specific for Lys^{27} of histone H3 and Lys^{26} of histone H1 (reviewed in ref. 22). Overexpression of EZH2 has been shown to induce a bypass of the cellular senescence program in mouse embryonic fibroblasts and to prevent mouse hematopoietic stem cell exhaustion (41). Conversely, transient knockdown of EZH2 in primary human fibroblasts and a variety of transformed cells inhibited their proliferation *in vitro* (42). EZH2 expression has been proposed to be controlled by the Rb-E2F pathway and to be a downstream mediator of E2F-dependent proliferation (42). High EZH2 expression that has been observed in a broad range of tumors has thus far been attributed either to Rb loss or gene amplification (42). Its silencing function is speculated to target tumor suppressor genes (43), but the precise mechanism of its action on cell proliferation has thus far not been elucidated.

Because of its role in stem cell maintenance and possibly tumor initiation (42, 44), we addressed the putative implication of *EZH2* in ESFT pathogenesis. The *EZH2* gene was found to be up-regulated in ESFT compared with normal tissues and neuroblastomas (21), and quantitative real-time PCR analysis confirmed *EZH2* induction in hMSC$^{EWS\text{-}FLI\text{-}1}$ as well as its dependence on EWS-FLI-1 DBD integrity (Fig. 4*A* and data not shown).

Expression of *EZH2* has been reported to progressively decrease during serial passage of primary fibroblasts and hematopoietic stem cells cultured *in vitro*, resulting in activation of their senescence program (42). We therefore asked whether the elevated *EZH2* expression observed in hMSC$^{EWS\text{-}FLI\text{-}1}$ was the result of true up-regulation or mere maintenance of *EZH2* transcripts at the level found in low-passage hMSCs. *EZH2* expression levels in two different batches of empty vector–, DBDM-, and EWS-FLI-1–infected hMSCs after 20 doublings were compared by real-time PCR with those in parental wt hMSCs after 8 doublings. A 50% decrease in *EZH2* expression was observed in cells infected with empty vector and the DBDM that had undergone 20 population doublings compared with parental wt cells that had undergone 8 doublings. By contrast, hMSC$^{EWS\text{-}FLI\text{-}1}$, after 20 doublings, showed a 6- to 7-fold induction of *EZH2* expression compared with their 8 population doubling wt counterparts (Fig. 4*A*). This result clearly shows the ability of EWS-FLI-1 to induce *EZH2* in hMSCs above the baseline level of their precursors that had undergone fewer population doublings, and is consistent with a possible role in both senescence prevention and stem cell maintenance in hMSCs.

We next tested Ewing's sarcoma samples and xenotransplants of Ewing's sarcoma cell lines for EZH2 expression and found it to be elevated in both primary Ewing's sarcoma and ESFT cell line–derived tumors grown in immunocompromised mice (Fig. 4*B*). To address the possible functional implication of EZH2 in Ewing's sarcoma growth, we relied on a stable shRNA knockdown approach in ESFT cell lines using two distinct RNAi sequences (shRNA1 and shRNA2). Stable EZH2 shRNA expression in A673 and SK-N-MC Ewing's sarcoma cell lines resulted in >70% reduction of its mRNA level (Fig. 4*C, left*) and a significant decrease in EZH2 protein expression as assessed by Western blot analysis (Fig. 4*C, right*). Reduction of EZH2 expression caused a marked decrease in proliferation of the two cell lines *in vitro* (Fig. 4*D*). Furthermore, injection of these cells into immunocompromised mice resulted in either no tumor development or strongly reduced tumor growth compared with cells expressing unrelated RNAi sequences (Fig. 5). To exclude possible off-target effects of the shRNA sequences, we repeated these experiments using two additional distinct shRNA sequences and obtained comparable results (data not shown).

Based on the notion that EZH2 may repress p16 and possibly other cell cycle regulators (43), we tested the expression level of several cell cycle control genes in the EZH2-depleted cells by real-time PCR. Both of the ESFT cell lines used in our experiments have a nonfunctional p53 pathway (45). The A673 cell line also lacks the p16^{INK4A}-p14^{ARF} locus whereas SK-N-MC cells express an inactive Rb protein but retain expression of wt p16^{INK4A}-p14^{ARF} (45).

Whether or not they were mutated, we did not record any significant change in the expression levels of $p14^{ARF}$, p15, $p16^{INK4A}$, p18, p21, and p53 following the EZH2 knockdown (data not shown). The observed reduction in proliferation and tumorigenicity can therefore not be explained by an effect on these cell cycle inhibitors and is most likely mediated by a mechanism that has yet to be elucidated.

Discussion

EWS-FLI-1 has thus far been found to induce an oncogenic stress type response in primary human cells, leading to cell cycle arrest, and a partial ESFT transcriptome in a variety of heterologous cell lines. Our present observations identify MSCs as the first primary human cell type that, while accurately recapitulating the ESFT gene expression profile, maintains viability and proliferation in response to EWS-FLI-1.

EWS-FLI-1 induced marked rounding of hMSCs *in vitro* that accompanied robust expression changes of genes implicated in cell differentiation. Consistent with previous studies in tumor cells and immortalized fibroblasts, microarray analysis revealed that numerous genes induced in $hMSC^{EWS\text{-}FLI\text{-}1}$ are implicated in neural crest development and neuronal differentiation. Among the most differentially expressed transcripts, we found NGFR (p75), which was strongly induced at both the transcription and protein levels, and which, in addition to playing a central role in neural develop-

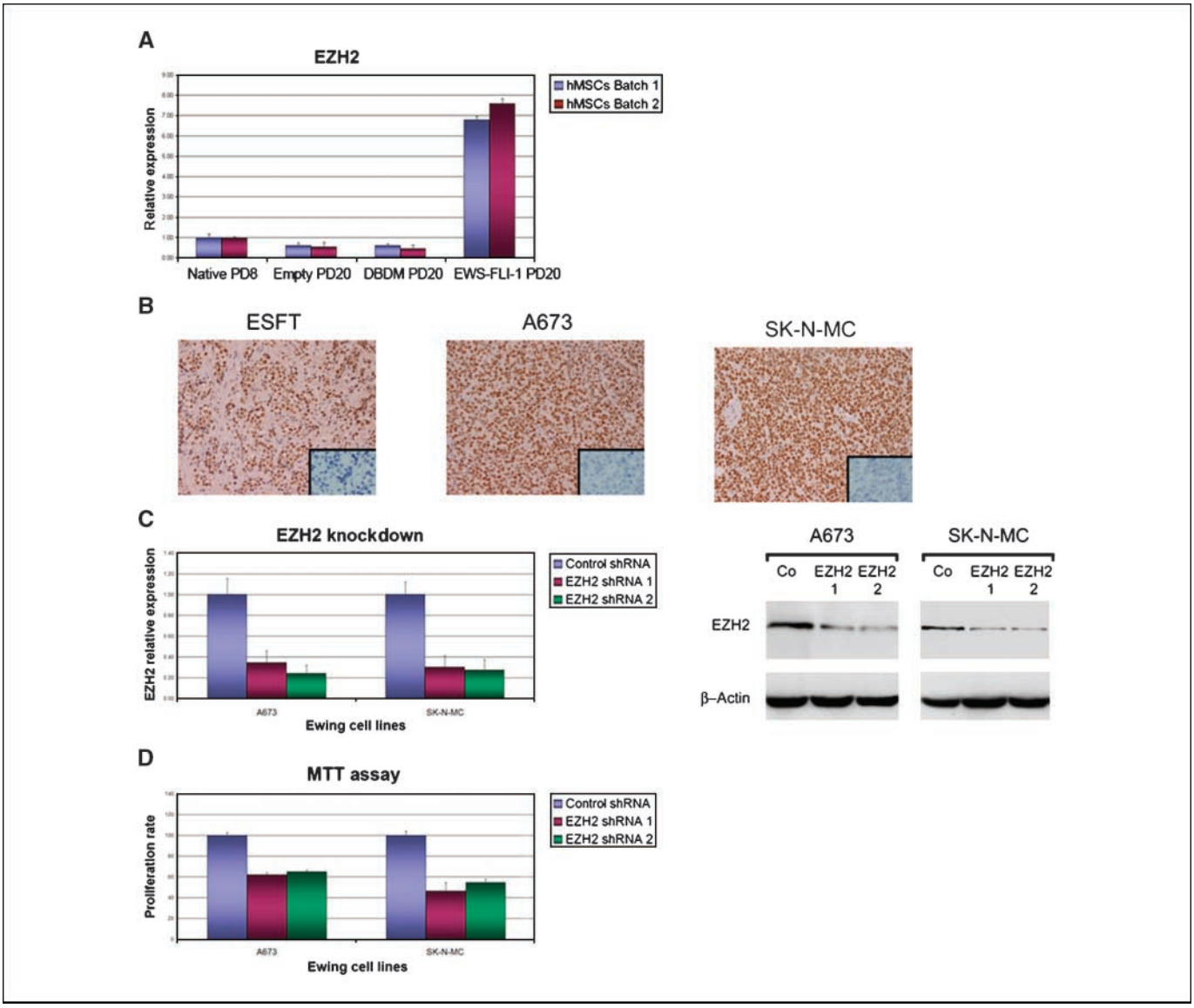

Figure 4. EZH2 is induced in $hMSC^{EWS\text{-}FLI\text{-}1}$ and expressed in ESFT, supporting tumor cell proliferation. *A,* EZH2 transcript induction in $hMSC^{EWS\text{-}FLI\text{-}1}$ compared with empty vector– and DBDM-infected cells at 20 population doublings and parental cells at 8 population doublings. *B,* immunohistochemical assessment of EZH2 expression in primary ESFT and cell line–derived tumors grown in immunocompromised mice. Magnification, ×100. *Inset,* staining with isotype-matched unrelated antibody. Magnification, ×200. *C,* real-time PCR (*left*) and Western blot analysis (*right*) of EZH2 expression knockdown following stable shRNA in A673 and SK-N-MC Ewing's sarcoma cell lines. The experiments were done with two different EZH2-specific (EZH2 shRNA1 and shRNA2) sequences and an unrelated siRNA control. Real-time PCR experiments were normalized to cyclophyllin A and done in triplicate. *Columns,* mean of three independent determinations; *bars,* SD. *D,* A673 and SK-N-MC cell proliferation rate is significantly reduced after the stable knockdown of EZH2 shown in *C. Columns,* mean of triplicate values of three separate determinations; *bars,* SD.

	shRNA	Nb mice inj.	Nb tumors	Median weight
A673	Control	6	6	1.5 (g)
	EZH2 sh RNA 1	6	3	0.8 (g)
	EZH2 sh RNA 2	6	4	0.8 (g)
SK-N-MC	Control	6	6	1.4 (g)
	EZH2 sh RNA 1	6	1	0.2 (g)
	EZH2 sh RNA 2	6	0	0.0 (g)

Figure 5. Reduction of EZH2 expression in A673 and SK-N-MC cell lines causes either no tumor development or reduced tumor growth compared with cells expressing unrelated RNAi sequences.

ment, is a key marker of neuroectodermal stem cells in both normal tissues and neural crest–derived tumors (46). Among the other genes that constitute part of the neuroectodermal profile of hMSC$^{EWS\text{-}FLI\text{-}1}$, *SOX2* has been shown to maintain neural progenitor features (47). In contrast to observations in mouse mesenchymal progenitor cells, which were reported to lose osteogenic and adipocytic differentiation potential as a result of EWS-FLI-1 expression, hMSCs expressing EWS-FLI-1 retained at least some degree of trilineage differentiation plasticity. It is plausible that the early-stage neuroectodermal differentiation program induced by EWS-FLI-1 in hMSCs can still be overridden by the supraphysiologic conditions of the *in vitro* differentiation assays.

Some of the genes that are implicated in neural differentiation have recently been suggested to play an active role in ESFT pathogenesis. Thus, *NROB1* can promote tumorigenesis of Ewing's sarcoma cell lines (7), whereas NKX2-2 may provide important functions at specific stages of ESFT development because its repression strongly reduced ESFT cell line tumorigenicity (10). It is noteworthy that both genes were not only strongly induced in hMSC$^{EWS\text{-}FLI\text{-}1}$ but also remained dependent on EWS-FLI-1 expression in established and tumorigenic ESFT cell lines. These observations suggest that they play a role not only during the initial steps of tumor development but also at late stages of tumor growth. Importantly, several of the above genes have been found to be strong discriminators of ESFT, and their expression has been used as an argument that ESFT may be of neuroectodermal origin. However, the present experiments show that expression of genes implicated in neuronal differentiation and neural crest development can be induced by EWS-FLI-1 in the appropriate primary mesenchymal progenitor cell environment. Thus, a hMSC that can undergo partial neuroectodermal differentiation may constitute the origin of ESFT, suggesting that these tumors need not arise from a neuroectodermal precursor to explain their primitive neuroectodermal phenotype.

Several of the genes observed to be up-regulated in hMSC$^{EWS\text{-}FLI\text{-}1}$ and expressed in ESFT have been proposed to be functionally related to Ewings' sarcoma development and behavior. Thus, *ID2*, observed to be induced by EWS-FLI-1 in both hMSCs and mouse mesenchymal progenitor cells (20), may play an important role in promoting cell cycle entry by inhibiting Rb. Induction of *fos* that was detected as a result of EWS-FLI-1 introduction into hMSCs (Supplementary data 1C) may be of particular interest in light of recent evidence that expression of numerous candidate EWS-FLI-1 target genes requires cooperation between EWS-FLI-1 and activator protein-1 (AP-1) (48). Enhanced expression of *fos* may explain, in part, the broad ESFT gene repertoire that was up-regulated in hMSC$^{EWS\text{-}FLI\text{-}1}$, and may therefore underlie the ability of these cells to recapitulate ESFT features. Moreover, and in contrast to primary fibroblasts, expression of EWS-FLI-1 in hMSCs did not provoke a p53 response, as shown by the absence of p53 target gene induction in their gene expression profile and the corresponding growth arrest. EWS-FLI-1 signals may either fail to activate premature cell senescence and oncogenic stress pathways, including p53 in hMSCs, or trigger mechanisms that neutralize or circumvent them.

Two candidate EWS-FLI-1 target genes that were induced in hMSC$^{EWS\text{-}FLI\text{-}1}$ and that may prevent cell senescence while promoting survival and proliferation are *IGF1* and *EZH2*. We have previously shown that *IGF1* is induced by EWS-FLI-1 in mouse mesenchymal progenitor cells (20). Coupled to that observation, the present findings suggest that *IGF1* may be an important EWS-FLI-1 target in MSCs. It is noteworthy that mouse mesenchymal progenitor cells and hMSCs are the only cells in which up-regulation of *IGF-I* by EWS-FLI-1 has been reported thus far. Although the direct or indirect nature of the effect remains to be determined, our experiments clearly indicate that the DNA binding ability of EWS-FLI-1 is required for *IGF1* induction in hMSCs. IGF-IR signaling is observed to be critical for ESFT growth, and its blockade induces growth arrest and apoptosis in ESFT cell lines (49). IGF-I induction may provide a survival signal that is essential during the initiating phases of tumor development, when the primary cells are subjected to the strong oncogenic stimulus of EWS-FLI-1 expression.

The discovery that *EZH2* is induced by EWS-FLI-1 in hMSCs may provide an additional explanation about why EWS-FLI-1 does not elicit oncogenic stress–mediated cell cycle arrest in hMSCs. Similar to another polycomb group gene, *bmi*-1, which cooperates with myc in B-cell and T-cell lymphoma development by inhibiting myc-induced apoptosis through repression of the *Cdkn2a* locus, *EZH2* activity is suggested to participate in blocking cellular response to oncogenic stress and maintain stem cell renewal at the expense of differentiation (22). *EZH2* has also been proposed to act as an oncogene in its own right (42) and to become up-regulated in preneoplastic lesions in the breast (44). Consistent with these scenarios, *EZH2* repression resulted in reduction of ESFT cell proliferation and tumorigenicity. Combined targeting of IGF-IR and EZH2 may provide an attractive therapeutic option in ESFT.

Taken together, our observations provide evidence for the first time that hMSCs can sustain EWS-FLI-1 expression and respond by adopting phenotypic and gene expression hallmarks of ESFT, as would be expected of its putative cell of origin. These results are supported by recent work reporting the appearance of MSC features in Ewing's sarcoma cell lines subjected to EWS-FLI-1 knockdown (50). As such, hMSC$^{EWS\text{-}FLI\text{-}1}$ may provide an ideal cellular environment for uncovering new candidate genes whose role in ESFT initiation and subsequent maintenance can be tested. Although tumor initiation by adult hMSCs may require a genetic event in addition to EWS-FLI-1 expression, the overall gene expression and phenotypic changes observed in response to EWS-FLI-1 alone argue that hMSC$^{EWS\text{-}FLI\text{-}1}$ constitutes a strong candidate precursor of ESFT.

Acknowledgments

Received 5/12/2007; revised 11/29/2007; accepted 1/24/2008.

Grant support: Fonds National de la Recherche Scientifique grant 3100A0-105833, Oncosuisse grant 01656-02-2005, and the National Center of Competence in Research Molecular Oncology (I. Stamenkovic).

The costs of publication of this article were defrayed in part by the payment of page charges. This article must therefore be hereby marked *advertisement* in accordance with 18 U.S.C. Section 1734 solely to indicate this fact.

We thank Prof. Pierre Hoffmeyer for fruitful collaboration and for providing surgical samples, Joan Stalder for technical support, and Carlo Fusco for insightful discussions.

References

1. Delattre O, Zucman J, Plougastel B, et al. Gene fusion with an ETS DNA-binding domain caused by chromosome translocation in human tumours. Nature 1992;359:162–5.
2. Eliazer S, Spencer J, Ye D, Olson E, Ilaria RL, Jr. Alteration of mesodermal cell differentiation by EWS/FLI-1, the oncogene implicated in Ewing's sarcoma. Mol Cell Biol 2003;23:482–92.
3. Hu-Lieskovan S, Zhang J, Wu L, Shimada H, Schofield DE, Triche TJ. EWS-FLI1 fusion protein up-regulates critical genes in neural crest development and is responsible for the observed phenotype of Ewing's family of tumors. Cancer Res 2005;65:4633–44.
4. May WA, Gishizky ML, Lessnick SL, et al. Ewing sarcoma 11;22 translocation produces a chimeric transcription factor that requires the DNA-binding domain encoded by FLI1 for transformation. Proc Natl Acad Sci U S A 1993;90:5752–6.
5. Rorie CJ, Thomas VD, Chen P, Pierce HH, O'Bryan JP, Weissman BE. The Ews/Fli-1 fusion gene switches the differentiation program of neuroblastomas to Ewing sarcoma/peripheral primitive neuroectodermal tumors. Cancer Res 2004;64:1266–77.
6. Thompson AD, Teitell MA, Arvand A, Denny CT. Divergent Ewing's sarcoma EWS/ETS fusions confer a common tumorigenic phenotype on NIH3T3 cells. Oncogene 1999;18:5506–13.
7. Kinsey M, Smith R, Lessnick SL. NR0B1 is required for the oncogenic phenotype mediated by EWS/FLI in Ewing's sarcoma. Mol Cancer Res 2006;4:851–9.
8. Mendiola M, Carrillo J, Garcia E, et al. The orphan nuclear receptor DAX1 is up-regulated by the EWS/FLI1 oncoprotein and is highly expressed in Ewing tumors. Int J Cancer 2006;118:1381–9.
9. Owen LA, Lessnick SL. Identification of target genes in their native cellular context: an analysis of EWS/FLI in Ewing's sarcoma. Cell Cycle 2006;5:2049–53.
10. Smith R, Owen LA, Trem DJ, et al. Expression profiling of EWS/FLI identifies NKX2.2 as a critical target gene in Ewing's sarcoma. Cancer Cell 2006;9:405–16.
11. May WA, Arvand A, Thompson AD, Braun BS, Wright M, Denny CT. EWS/FLI1-induced manic fringe renders NIH 3T3 cells tumorigenic. Nat Genet 1997;17:495–7.
12. Kovar H, Aryee DN, Jug G, et al. EWS/FLI-1 antagonists induce growth inhibition of Ewing tumor cells *in vitro*. Cell Growth Differ 1996;7:429–37.
13. Tanaka K, Iwakuma T, Harimaya K, Sato H, Iwamoto Y. EWS-Fli1 antisense oligodeoxynucleotide inhibits proliferation of human Ewing's sarcoma and primitive neuroectodermal tumor cells. J Clin Invest 1997;99:239–47.
14. Prieur A, Tirode F, Cohen P, Delattre O. EWS/FLI-1 silencing and gene profiling of Ewing cells reveal downstream oncogenic pathways and a crucial role for repression of insulin-like growth factor binding protein 3. Mol Cell Biol 2004;24:7275–83.
15. Riggi N, Stamenkovic I. The Biology of Ewing sarcoma. Cancer Lett 2007;254:1–10.
16. Deneen B, Denny CT. Loss of p16 pathways stabilizes EWS/FLI1 expression and complements EWS/FLI1 mediated transformation. Oncogene 2001;20:6731–41.
17. Lessnick SL, Dacwag CS, Golub TR. The Ewing's sarcoma oncoprotein EWS/FLI induces a p53-dependent growth arrest in primary human fibroblasts. Cancer Cell 2002;1:393–401.
18. Huang HY, Illei PB, Zhao Z, et al. Ewing sarcomas with p53 mutation or p16/p14ARF homozygous deletion: a highly lethal subset associated with poor chemoresponse. J Clin Oncol 2005;23:548–58.
19. Castillero-Trejo Y, Eliazer S, Xiang L, Richardson JA, Ilaria RL, Jr. Expression of the EWS/FLI-1 oncogene in murine primary bone-derived cells Results in EWS/FLI-1-dependent, Ewing sarcoma-like tumors. Cancer Res 2005;65:8698–705.
20. Riggi N, Cironi L, Provero P, et al. Development of Ewing's sarcoma from primary bone marrow-derived mesenchymal progenitor cells. Cancer Res 2005;65:11459–68.
21. Staege MS, Hutter C, Neumann I, et al. DNA microarrays reveal relationship of Ewing family tumors to both endothelial and fetal neural crest-derived cells and define novel targets. Cancer Res 2004;64:8213–21.
22. Sparmann A, van Lohuizen M. Polycomb silencers control cell fate, development and cancer. Nat Rev Cancer 2006;6:846–56.
23. Suva D, Garavaglia G, Menetrey J, et al. Non-hematopoietic human bone marrow contains long-lasting, pluripotential mesenchymal stem cells. J Cell Physiol 2004;198:110–8.
24. Suva D, Passweg J, Arnaudeau S, Hoffmeyer P, Kindler V. *In vitro* activated human T lymphocytes very efficiently attach to allogenic multipotent mesenchymal stromal cells and transmigrate under them. J Cell Physiol 2008;214:588–94.
25. Welford SM, Hebert SP, Deneen B, Arvand A, Denny CT. DNA binding domain-independent pathways are involved in EWS/FLI1-mediated oncogenesis. J Biol Chem 2001;276:41977–84.
26. Torchia EC, Jaishankar S, Baker SJ. Ewing tumor fusion proteins block the differentiation of pluripotent marrow stromal cells. Cancer Res 2003;63:3464–8.
27. Breitling R, Armengaud P, Amtmann A, Herzyk P. Rank products: a simple, yet powerful, new method to detect differentially regulated genes in replicated microarray experiments. FEBS Lett 2004;573:83–92.
28. Deneen B, Hamidi H, Denny CT. Functional analysis of the EWS/ETS target gene uridine phosphorylase. Cancer Res 2003;63:4268–74.
29. Fuchs B, Inwards CY, Janknecht R. Up-regulation of the matrix metalloproteinase-1 gene by the Ewing's sarcoma associated EWS-ER81 and EWS-Fli-1 oncoproteins, c-Jun and p300. FEBS Lett 2003;553:104–8.
30. Watanabe G, Nishimori H, Irifune H, et al. Induction of tenascin-C by tumor-specific EWS-ETS fusion genes. Genes Chromosomes Cancer 2003;36:224–32.
31. Baird K, Davis S, Antonescu CR, et al. Gene expression profiling of human sarcomas: insights into sarcoma biology. Cancer Res 2005;65:9226–35.
32. Henderson SR, Guiliano D, Presneau N, et al. A molecular map of mesenchymal tumors. Genome Biol 2005;6:R76.
33. Codrington R, Pannell R, Forster A, et al. The Ews-ERG fusion protein can initiate neoplasia from lineage-committed haematopoietic cells. PLoS Biol 2005;3:e242.
34. Perez-Losada J, Pintado B, Gutierrez-Adan A, et al. The chimeric FUS/TLS-CHOP fusion protein specifically induces liposarcomas in transgenic mice. Oncogene 2000;19:2413–22.
35. Riggi N, Cironi L, Provero P, et al. Expression of the FUS-CHOP fusion protein in primary mesenchymal progenitor cells gives rise to a model of myxoid liposarcoma. Cancer Res 2006;66:7016–23.
36. Funes JM, Quintero M, Henderson S, et al. Transformation of human mesenchymal stem cells increases their dependency on oxidative phosphorylation for energy production. Proc Natl Acad Sci U S A 2007;104:6223–8.
37. Kennedy JA, Barabe F, Patterson BJ, et al. Expression of TEL-JAK2 in primary human hematopoietic cells drives erythropoietin-independent erythropoiesis and induces myelofibrosis *in vivo*. Proc Natl Acad Sci U S A 2006;103:16930–5.
38. Pereira DS, Dorrell C, Ito CY, et al. Retroviral transduction of TLS-ERG initiates a leukemogenic program in normal human hematopoietic cells. Proc Natl Acad Sci U S A 1998;95:8239–44.
39. Bracken AP, Dietrich N, Pasini D, Hansen KH, Helin K. Genome-wide mapping of Polycomb target genes unravels their roles in cell fate transitions. Genes Dev 2006;20:1123–36.
40. Caretti G, Di Padova M, Micales B, Lyons GE, Sartorelli V. The Polycomb Ezh2 methyltransferase regulates muscle gene expression and skeletal muscle differentiation. Genes Dev 2004;18:2627–38.
41. Kamminga LM, Bystrykh LV, de Boer A, et al. The Polycomb group gene Ezh2 prevents hematopoietic stem cell exhaustion. Blood 2006;107:2170–9.
42. Bracken AP, Pasini D, Capra M, Prosperini E, Colli E, Helin K. EZH2 is downstream of the pRB-E2F pathway, essential for proliferation and amplified in cancer. EMBO J 2003;22:5323–35.
43. Kotake Y, Cao R, Viatour P, Sage J, Zhang Y, Xiong Y. pRB family proteins are required for H3K27 trimethylation and Polycomb repression complexes binding to and silencing p16INK4α tumor suppressor gene. Genes Dev 2007;21:49–54.
44. Ding L, Kleer CG. Enhancer of zeste 2 as a marker of preneoplastic progression in the breast. Cancer Res 2006;66:9352–5.
45. Kovar H, Jug G, Aryee DN, et al. Among genes involved in the RB dependent cell cycle regulatory cascade, the p16 tumor suppressor gene is frequently lost in the Ewing family of tumors. Oncogene 1997;15:2225–32.
46. Stemple DL, Anderson DJ. Isolation of a stem cell for neurons and glia from the mammalian neural crest. Cell 1992;71:973–85.
47. Graham V, Khudyakov J, Ellis P, Pevny L. SOX2 functions to maintain neural progenitor identity. Neuron 2003;39:749–65.
48. Kim S, Denny CT, Wisdom R. Cooperative DNA binding with AP-1 proteins is required for transformation by EWS-Ets fusion proteins. Mol Cell Biol 2006;26:2467–78.
49. Scotlandi K, Avnet S, Benini S, et al. Expression of an IGF-I receptor dominant negative mutant induces apoptosis, inhibits tumorigenesis and enhances chemosensitivity in Ewing's sarcoma cells. Int J Cancer 2002;101:11–6.
50. Tirode F, Laud-Duval K, Prieur A, Delorme B, Charbord P, Delattre O. Mesenchymal stem cell features of Ewing tumors. Cancer Cell 2007;11:421–9.